PROTEINS
STRUCTURE ■ FUNCTION ■ BIOINFORMATICS

Mapping α-helical induced folding within the intrinsically disordered C-terminal domain of the measles virus nucleoprotein by site-directed spin-labeling EPR spectroscopy

Valérie Belle,[1†] Sabrina Rouger,[2†] Stéphanie Costanzo,[2] Elodie Liquière,[2] Janez Strancar,[3] Bruno Guigliarelli,[1] André Fournel,[1*] and Sonia Longhi[1*]

[1] Bioénergétique et Ingénierie des Protéines, UPR 9036 CNRS et Université Aix-Marseille I et II, 31 Chemin Joseph Aiguier, 13402 Marseille Cedex 9, France

[2] Architecture et Fonction des Macromolécules Biologiques, UMR 6098 CNRS et Universités Aix-Marseille I et II, Campus de Luminy, 13288 Marseille Cedex 9, France

[3] Department of Solid State Physics, "Josef Stefan" Institute, SI-1000 Ljubljana, Slovenia

ABSTRACT

Using site-directed spin-labeling EPR spectroscopy, we mapped the region of the intrinsically disordered C-terminal domain of measles virus nucleoprotein (N_{TAIL}) that undergoes induced folding. In addition to four spin-labeled N_{TAIL} variants (S407C, S488C, L496C, and V517C) (Morin et al. (2006), J Phys Chem 110: 20596-20608), 10 new single-site cysteine variants were designed, purified from *E. coli*, and spin-labeled. These 14 spin-labeled variants enabled us to map in detail the gain of rigidity of N_{TAIL} in the presence of either the secondary structure stabilizer 2,2,2-trifluoroethanol or the C-terminal domain X (XD) of the viral phosphoprotein. Different regions of N_{TAIL} were shown to contribute to a different extent to the binding to XD, while the mobility of the spin labels grafted at positions 407 and 460 was unaffected upon addition of XD; that of the spin labels grafted within the 488–502 and the 505–522 regions was severely and moderately reduced, respectively. Furthermore, EPR experiments in the presence of 30% sucrose allowed us to precisely map to residues 488–502, the N_{TAIL} region undergoing α-helical folding. The mobility of the 488–502 region was found to be restrained even in the absence of the partner, a behavior that could be accounted for by the existence of a transiently populated folded state. Finally, we show that the restrained motion of the 505–522 region upon binding to XD is due to the α-helical transition occurring within the 488–502 region and not to a direct interaction with XD.

Proteins 2008; 73:973–988.

Key words: intrinsic disorder; induced folding; disorder-to-order transitions; residual structure; conformer selection; spin labeling; EPR spectroscopy; measles virus; nucleoprotein; phosphoprotein.

INTRODUCTION

Intrinsically disordered proteins (IDPs) are ubiquitary proteins that fulfill essential biological functions while being devoid of highly populated and uniform secondary and tertiary structure under physiological conditions in isolation.[1–7] Although there are IDPs that carry out their function while remaining permanently disordered (e.g. entropic chains),[1] many of them undergo induced folding, that is, a disorder-to-order transition upon binding to their physiological partners.[7–12] Noteworthy, these disorder-to-order transitions can be accompanied or not by the gain of regular secondary structure elements.[6,7,10,13,14]

IDPs do not constitute a uniform family and embrace extended conformations (random coil-like) as well as globally-collapsed conformations (molten globule-like).[15] Conformational and spectroscopic analyses showed that random coil-like proteins can in their turn be subdivided into two major groups: one consisting of proteins with extended maximum dimensions typical of random coils with no (or little) secondary structure, and one comprising the so-called premolten globules, which are more compact (but still less compact than

Abbreviations: CD, circular dichroism; EPR, electron paramagnetic resonance; IDP, intrinsically disordered protein; IPTG, isopropyl β-D-thiogalactopyranoside; L, large protein; MoRE, molecular recognition element; MTSL, methanethiosulfonate; MV, measles virus; N, nucleoprotein; NMR, nuclear magnetic resonance; NR, nucleoprotein receptor; P, phosphoprotein; PCR, polymerase chain reaction; PMSF, phenyl-methyl-sulfonyl-fluoride; R_S, stokes radius; SDSL, site-directed spin-labeling; TFE, 2,2,2-trifluoroethanol; XD, X domain of P.

Grant sponsors: Agence Nationale de la Recherche; Grant number: ANR-05-MIIM-035-02; National Institute of Neurological Disorders and Stroke; Grant number: R01 NS031693-11A2; Centre National de la Recherche Scientifique and the COST P15 action.
[†]Valérie Belle and Sabrina Rouger contributed equally to this work.
*Correspondence to: Sonia Longhi, AFMB, UMR 6098, 163, avenue de Luminy, Case 932, 13288 Marseille Cedex 09, France. E-mail: Sonia.Longhi@afmb.univ-mrs.fr or André Fournel, BIP, UPR 9036 CNRS, 31 Chemin Joseph Aiguier, 13402 Marseille Cedex, France. E-mail: fournel@ibsm.cnrs-mrs.fr
Received 10 February 2008; Revised 4 April 2008; Accepted 22 April 2008
Published online 5 June 2008 in Wiley InterScience (www.interscience.wiley.com).
DOI: 10.1002/prot.22125

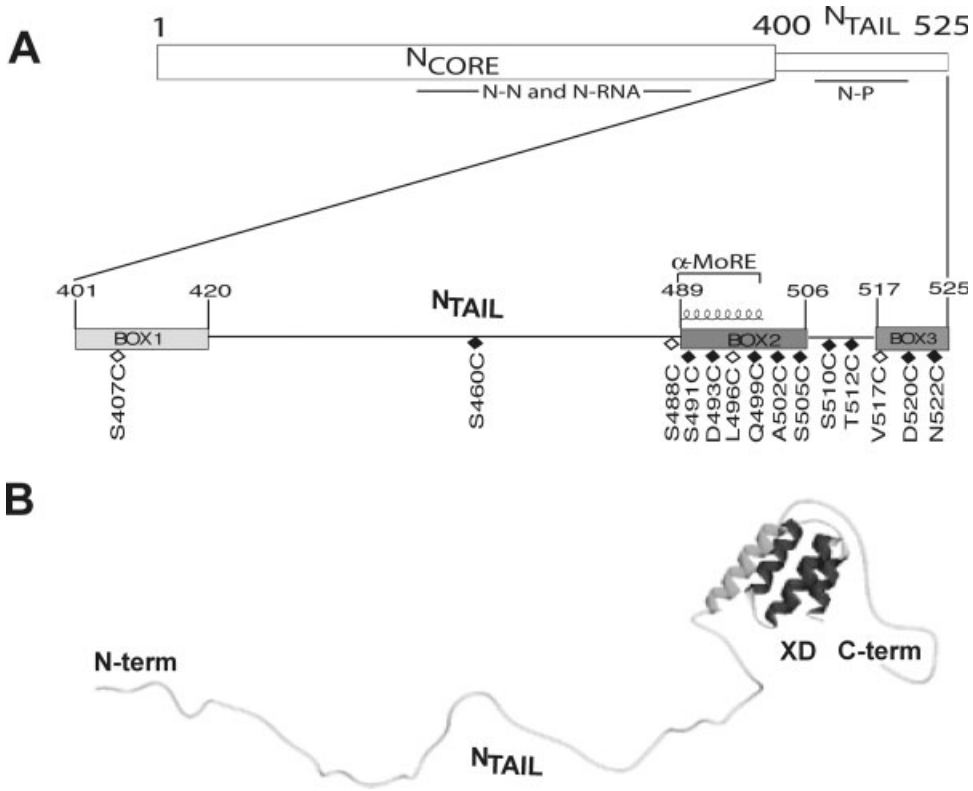

Figure 1

(**A**) Organization of the N protein and schematic representation of positions targeted for cysteine substitution and spin-labeling (diamonds). Positions targeted in this work are represented by black diamonds, while those targeted in our previously published study[24] are shown in white. (**B**) Model of the N_{TAIL}-XD complex as derived by small-angle X-ray scattering studies, highlighting the involvement of the α-MoRE and of the C-terminus of N_{TAIL} (Box3) in the interaction with XD.[14]

globular or molten globule proteins) and conserve some residual secondary structure.[1,3] It has been proposed that the residual intramolecular interactions that typify the premolten globule state may enable a more efficient start of the folding process induced by a partner.[2,11,16–18]

Measles virus (MV) is an enveloped RNA virus within the *Morbillivirus* genus of the *Paramyxoviridae* family. Its nonsegmented, negative-sense, single-stranded RNA genome is encapsidated by the viral nucleoprotein (N) within a helical nucleocapsid. This latter is the substrate used by the viral polymerase complex during transcription and replication. The viral polymerase complex consists of the large protein (L) and of the phosphoprotein (P) that is an essential polymerase cofactor as it tethers the L protein onto the nucleocapsid template.

The MV nucleoprotein consists of two regions: a structured N-terminal moiety, N_{CORE} (aa 1–400), which contains all the regions necessary for self-assembly and RNA-binding,[19,20] and a C-terminal domain, N_{TAIL} (aa 401–525) that is intrinsically unstructured[21] and exposed at the surface of the viral nucleocapsid[19,22,23] [Fig. 1(A)]. Because of its intrinsic flexible nature, N_{TAIL} interacts with various partners, including host cell proteins, such as Hsp72,[25,26] a cellular receptor referred to as Nucleoprotein Receptor[27,28] and the P protein.[20,21]

The P protein has a modular organization.[29,30] We have previously reported the crystal structure of the C-terminal X domain (XD, aa 459–507) of P, and shown by circular dichroism that XD is responsible for the α-helical folding of N_{TAIL}.[31] Within a conserved region of N_{TAIL} (aa 489–506, Box2), an α-helical molecular recognition element (α-MoRE, aa 489–499) involved in binding to P and in induced folding was identified[32] and modeled in the crystal structure of XD.[31] This model has been successively validated by Kingston *et al.* who solved the crystal structure of a chimeric construct consisting of XD and of the 486–504 region of N_{TAIL}.[33] Using small angle X-ray scattering, we have obtained a low-resolution structural model of the complex between XD and the entire N_{TAIL} domain[14] [Fig. 1(B)]. This model shows that most of N_{TAIL} (residues 401–488) remains disordered in the complex and does not establish contacts with XD. It also provides evidence for the involvement of the N_{TAIL} region downstream the α-MoRE in binding to XD. That N_{TAIL} possesses an additional site (Box3, aa 517–525) involved in the interaction with XD has been

further confirmed by several approaches, including surface plasmon resonance, circular dichroism, and NMR spectroscopy.[14] However, although the N_{TAIL}–XD interaction has been the focus of numerous studies (for reviews, see Refs. 34–36) only partial structural information on the N_{TAIL}–XD complex is presently available. Indeed, crystallographic data have been obtained on a chimera construct containing only 18 out of 125 N_{TAIL} residues,[33] and NMR studies carried out with the entire N_{TAIL} domain and XD did not provide full structural information because of the lack of assignment of the N_{TAIL} HSQC spectrum.[14] On the other hand, CD and SAXS data[14] only provided global and low-resolution structural information, respectively.

In this study, we used a complementary approach, namely site-directed spin-labeling (SDSL) coupled to electron paramagnetic resonance (EPR) spectroscopy, to investigate the induced folding of N_{TAIL} in solution. This technique provides information at the residue level. Indeed, it relies on the introduction of a paramagnetic spin label through covalent modification of a unique sulfydryl group using a selective nitroxide reagent and on the ensuing monitoring of variations in the spin label mobility under various conditions. The advantage of this technique is that paramagnetic probes introduce a minimal perturbation of the system, and that it probes the very local environment of the spin label.[37–40]

We have previously reported a study where the N_{TAIL}–XD interaction has been investigated by SDSL EPR spectroscopy. In this previous study, we targeted four different N_{TAIL} sites for spin-labeling [see Fig. 1(A)] and showed that SDSL EPR spectroscopy is a well suited method to assess the induced folding events that N_{TAIL} undergoes in the presence of either the secondary structure stabilizer 2,2,2-trifluoroethanol (TFE) or XD.[24]

To more precisely map the α-helical folding that N_{TAIL} undergoes in the presence of XD, and to achieve a better understanding of the molecular mechanisms governing this folding process, we targeted for spin-labeling 10 additional N_{TAIL} sites, 9 of which are scattered in the 488–525 region, while 1 (position 460) is located outside the reported region of interaction with XD [Fig. 1(A)]. We then recorded EPR spectra in the presence of either TFE or XD (both either in the absence or in the presence of 30% sucrose). We show that different regions of N_{TAIL} contribute to a different extent to the interaction with XD and propose a model for the molecular mechanism of XD-induced folding of N_{TAIL}.

MATERIALS AND METHODS

Construction of protein expression plasmids

The XD gene construct, encoding residues 459–507 of the MV P protein (strain Edmonston B) with an hexahistidine tag fused to its C-terminus, has already been described.[31]

All N_{TAIL} constructs were obtained by PCR (polymerase chain reaction) using as template the plasmid pDest14/N_{TAILHN},[14] which encodes residues 401–525 of the MV N protein (strain Edmonston B) with a hexahistidine tag fused to its N-terminus. Each mutant construct was obtained using *Turbo-Pfu* polymerase (Stratagene) and a pair of complementary mutagenic primers of 39 nucleotides in length (Operon). PCR cycles were carried out according to the supplier's instructions. After digestion with *Dpn*I to remove the methylated DNA template, transformation of *E. coli* strain DH10β (Stratagene) with the amplified PCR product was carried out. Primers were all designed to introduce a Cys codon, as well as to either bring in or suppress a restriction site in a silent manner, thus allowing discrimination of candidate clones from parental (*Dpn*I-undigested) clones after transformation. Specifically, an *Xho*I, a *Nde*I, a *BamH*I, and a *Pst*I restriction site was introduced in N_{TAIL} S460C, N_{TAIL} S505C, N_{TAIL} T512C, and N_{TAIL} D520C constructs, respectively, while the *Pvu*II site of N_{TAIL} S491C and D493C constructs, the *Nco*I site of N_{TAIL} Q499C and A502C constructs, and the *Xba*I site of the N_{TAIL} N522C construct were suppressed. The sequence of the N_{TAIL} coding region of all expression plasmids was verified by sequencing (GenomeExpress, France).

Expression of N_{TAIL} constructs

E. coli strain Rosetta [DE3] (Novagen) was used for the expression of N_{TAIL} mutants. Since the MV N gene contains several rare codons that are used with a very low frequency in *E. coli*, coexpression of N_{TAIL} constructs with the plasmid pLysS (Novagen) was carried out. This plasmid, which supplies six rare tRNAs, carries also the lysozyme gene, thus allowing a tight regulation of the expression of the recombinant gene, as well as a facilitated lysis. Cultures were grown overnight to saturation in Luria-Bertani (LB) medium containing 100 μg/mL ampicilin and 17 μg/mL chloramphenicol. An aliquot of the overnight culture was diluted 1/25 in LB medium and grown at 37°C. At OD_{600} of 0.7, isopropyl β-D-thiogalactopyranoside (IPTG) was added to a final concentration of 0.2 m*M*, and the cells were grown at 37°C for 3 h. The induced cells were harvested, washed and collected by centrifugation. The resulting pellets were frozen at −20°C.

Expression of tagged XD was carried out as described in Ref. 31. Expression of hexahistidine tagged *wt* N_{TAIL} (N_{TAIL}) was carried out as described in Ref. 14.

Purification of N_{TAIL} variant proteins

Cellular pellets from bacteria transformed with the different N_{TAIL} expression plasmids were resuspended in 5 Vol. (v/w) of buffer A (50 m*M* sodium phosphate pH 8,

300 m*M* NaCl, 10 m*M* Imidazole, 1 m*M* phenyl-methyl-sulfonyl-fluoride (PMSF)[1]) supplemented with 0.1 mg/mL lysozyme, 10 μg/mL DNAse I, protease inhibitor cocktail (Roche, one tablet per 50 mL of lysis buffer). After a 20-min incubation with gentle agitation, the cells were disrupted by sonication using a 750-W sonicator and four cycles of 30 s each at 60% power output. The lysate was clarified by centrifugation at 30,000*g* for 30 min. Starting from a 0.5-L culture, the clarified supernatant was incubated for 1 h with gentle shaking with 2 mL Chelating Sepharose Fast Flow Resin preloaded with Ni^{2+} ions (GE Healthcare), previously equilibrated in buffer A. The resin was washed with buffer A containing 20 m*M* imidazole, and the N_{TAIL} proteins were eluted in buffer A containing 250 m*M* imidazole. Eluates were analyzed by SDS-PAGE for the presence of the desired product. The fractions containing the recombinant product were combined, and concentrated using Centricon Plus-20 (molecular cutoff: 5000 Da, Millipore). The proteins were then loaded onto a Superdex 75 HR 10/30 column (GE Healthcare) and eluted in 10 m*M* sodium phosphate pH 7. The proteins were stored at −20°C. The purified N_{TAIL} protein variants are named according the amino acid substitution they bear.

Purification of histidine-tagged XD and *wt* N_{TAIL} was carried out as described in Refs. 14 and 31.

All purification steps, except for gel filtrations, were carried out at 4°C. Apparent molecular mass of proteins eluted from gel filtration columns was deduced from a calibration curve established with low molecular weight (LMW) and high molecular weight (HMW) calibration kits (GE Healthcare). The theoretical Stokes radii (R_s) of native (R_sN) and fully unfolded (R_sU) proteins were calculated according to Ref. 41.

Determination of protein concentration

Protein concentrations were either calculated using OD_{280} measurements and the theoretical absorption coefficients ϵ (mg/mL cm) at 280 nm as obtained using the program ProtParam at the EXPASY server (http://www.expasy.ch/tools), or measured using the Biorad protein assay (Bio-Rad).

Spin-labeling

Before spin-labeling, DTT was added to each purified N_{TAIL} mutated protein (~5 mg) in a one-hundred molar excess, except for the Q499C and A502C variants for which an excess of 1000 was used. The mixture was incubated for 30 min in an ice bath in order to reduce the unique free cysteine residue. DTT was removed by gel filtration onto a Superdex 75 HR 10/30 column (GE Healthcare) with 10 m*M* MES, 150 m*M* NaCl at pH 6.5 as elution buffer. The fractions containing the protein were pooled and then concentrated by ultrafiltration using Centricon Plus-20 (molecular cut-off: 5000 Da) (Millipore). The spin label (1-oxyl-2,2,5,5-tetramethyl-Δ3-pyrroline-3-methyl methane-thiosulfonate, MTSL, Toronto Research Chemicals Inc., Toronto, Canada) was immediately added to the concentrated sample at a molar excess of 10 using a spin label stock solution at 10 mg/mL in acetonitrile. The reaction was carried out during 1 h in the dark and in an ice bath, under gentle stirring and a continuous flow of argon to avoid oxydation. The excess of unbound spin label was removed by gel filtration as described above, except that 10 m*M* sodium phosphate at pH 7 was used as elution buffer. The fractions containing the labeled protein were pooled and concentrated as described above.

EPR spectroscopy and data analysis

EPR spectra were recorded at 296 K (± 0.2 K) on an ESP 300E Bruker spectrometer equipped with an ELEXSYS Super High Sensitivity resonator operating at 9.9 GHz. Samples were injected in a quartz capillary, whose sensible volume was about 20 μL. Protein concentrations in the 20–100 μ*M* range were used to record EPR spectra. The microwave power was 10 mW and the magnetic field modulation frequency and amplitude were 100 kHz and 0.1 mT, respectively.

The concentration of labeled proteins was evaluated by double integration of the EPR signal recorded under non-saturating conditions and comparison with that given by a 3-carboxy-proxyl standard sample. The labeling yields were estimated by calculating the ratio between the concentration of labeled proteins and the total protein concentration estimated as above described.

In this study, all EPR spectra (except for the position 491, see below) show that the nitroxide probe is in the so-called fast regime of mobility, with an outer line splitting remaining at $2\overline{A} = 3.2$ mT, where $\overline{A}$ is the average value of the hyperfine interaction. In our previous paper,[24] we have shown that these spectra can be well simulated by a model based on the calculation of line broadening in the case of a fast anisotropic rotational movement.[42] We showed that the most sensitive parameter to describe the mobility of the spin probe is the peak-to-peak amplitude of the low- and central-field lines, referred to as $h(+1)/h(0)$ as compared to the $h(-1)/h(0)$ ratio which is more appropriate when the spin label has an isotropic movement.[24] Another parameter often used to describe the spin label mobility is the linewidth measurement of the central line δ.[43] However, this latter parameter is less sensitive than the $h(+1)/h(0)$ ratio in the high mobility regime (data not shown).

In the case of the spin-labeled S491C N_{TAIL} variant in the presence of XD, the $h(+1)/h(0)$ ratio is no longer a reliable parameter of the radical mobility due to the restriction of the available space experienced by the label at this particular position. In the presence of XD, the

EPR spectrum of this particular variant contains two spectral components: one corresponding to N_{TAIL} bound to XD and the other corresponding to N_{TAIL} free in solution. The percentage of bound form in the presence of saturating amounts of XD was calculated as follows: (i) the spectrum of free S491C labeled protein was subtracted to the composite spectrum so as to obtain the one-component spectrum corresponding to the spin labeled S491C/XD complex (the bound form of the labeled protein), (ii) the integrated intensity of the resulting spectrum, I_{bound}, and of the composite, observed spectrum, I_{total}, were calculated and (iii) the proportion of the bound form was calculated as the I_{bound}/I_{total} ratio. The error in this determination was estimated to be 5%.

Equilibrium displacement experiments

To obtain an "EPR-silenced," hydroxylamine derivative of the S460C N_{TAIL} variant to be used in equilibrium displacement experiments, we reduced the spin-labeled S460C N_{TAIL} protein by incubating it in the presence of a 100-fold molar excess of ascorbic acid for 90 min at 25°C in 10 m*M* sodium phosphate pH 7. Reduction of the nitroxide to a hydroxylamine was assessed based on the flattening of the EPR signal. A residual EPR signal, corresponding to 10% of the original one, was found to persist even upon prolonged incubations. Ascorbic acid was then removed through a purification step onto a NAP-5 column (GE Healthcare). The protein was eluted with 10 m*M* sodium phosphate pH 7 and concentrated as described above.

Equilibrium displacement experiments were carried out with 40 μ*M* of spin-labeled L496C, 80 μ*M* of XD, and 40 μ*M* of reduced, hydroxylamine-labeled S460C to yield 1:2:1 protein mixtures. After subtracting the residual EPR signal persisting with reduced S460C, the resulting spectrum was composed of two signals: one arising from the free L496C spin-labeled protein and one resulting from the L496C spin-labeled protein bound to XD. The percentage of complex was inferred from the $[h(+1)/h(0)]_{mixture}$ ratio using a calibration curve obtained from the calculation of composite spectra corresponding to mixtures of unbound and 100% bound spin-labeled L496C. The error in this determination was estimated to be 5%. Note that, in this case, $[h(+1)/h(0)]_{mixture}$ is not an indicator of spin label mobility but a parameter for quantifying the proportion of the bound form in the N_{TAIL}-XD complex.

Circular dichroism

Circular dichroism (CD) spectra were recorded on a Jasco 810 dichrograph using 1-mm-thick quartz cells in 10 m*M* sodium phosphate pH 7 at 20°C.

Structural variations of N_{TAIL} proteins were measured as a function of changes in the initial CD spectrum upon addition of 20% TFE. CD spectra were measured between 185 and 260 nm, at 0.2 nm/min and were averaged from three scans. Moreover, each CD spectrum is the mean of three independent measurements so as to estimate the experimental error arising from sample preparation. The spectra were corrected for buffer signal and smoothed by using a third-order least square polynomial fit. Finally, mean ellipticity values per residue ($[\Theta]$) were calculated as $[\Theta] = 3300 \times m\ \Delta A/(l \times c \times n)$, where l (path length) = 0.1 cm, n = number of residues, m = molecular mass in Daltons, and c = protein concentration expressed in mg/mL. Number of residues (n) is 132 for all N_{TAIL} proteins, while m is ~14,600 Da for all N_{TAIL} variants. Protein concentrations of 0.1 mg/mL were used. The α-helical content was derived from the ellipticity at 222 nm as described in Ref. 44.

RESULTS

Rational design of N_{TAIL} cysteine-substituted variants

As previous computational, biochemical and crystallographic studies pointed out the formation of an α-helix within the Box2 region of N_{TAIL} upon binding to XD,[14,32,33] our goal was not to demonstrate the existence of the α-helical folding but rather to map its extent within the Box2–Box3 region. Hence, positions were not chosen so as to target each residue along the chain and to report the periodicity of the parameter describing the mobility of the spin probe[45] but rather to scatter their positions in different regions of interest.

We herein targeted for spin-labeling 10 additional different sites within N_{TAIL}, 1 located in the linker region between Box1 and Box2 (position 460), 5 within Box2 (positions 491, 493, 499, 502, and 505), 2 within the linker region between Box2 and Box3 (positions 510 and 512), and 2 within Box3 (positions 520 and 522) [Fig. 1(A)]. The rationale for the choice of a position in the middle of the region connecting Box1–Box2 was that no direct information was available on the possible involvement of the region connecting Box1–Box2 in binding to XD. Indeed, previous studies focused on the use of truncated N_{TAIL} proteins devoid of either Box3 ($N_{TAIL\Delta3}$, aa 401–516), or Box2 *plus* Box3 ($N_{TAIL\Delta2,3}$, aa 401–487), or Box1 ($N_{TAIL\Delta1}$, aa 421–525), showed that while Box2 and Box3 are affected by the addition of XD, Box1 is not.[14] However, these studies did not rule out a possible involvement of the region downstream Box1 in the interaction with XD.

Whenever possible, serine to cysteine substitutions were done. Ser460 was chosen so as to introduce the spin label in the middle of the region connecting Box1–Box2 [Fig. 1(A)]. However, isosteric substitution was not the sole criterion we used to target the various positions. In fact, in the case of Box2, the rationale for the choice of

positions was to scatter the spin probes as much as possible within the α-helix, while targeting residues whose side chains point towards the solvent within the chimeric complex between XD and the α-MoRE of N_{TAIL} (pdb code: 1T6O)[33] so as to avoid steric hindrance. The only exception is represented by position 491, whose side chain is buried at the interface of interaction in the crystal structure of the chimera (Fig. 2). The rationale for this choice was to assess whether the introduction of the spin label abrogated the ability of N_{TAIL} to form a complex with XD. Contrary to Box2, no high-resolution structural data are available for the 505–525 region, as the chimeric construct only contains residues 486–504 of N_{TAIL}. Hence, we targeted Ser510 and Thr512 for isosteric cysteine substitution within the region connecting Box2–Box3. Finally, as no serine residue occurs within Box3, positions 520 and 522 were chosen only on the basis of the spin label scattering criterion [Fig. 1(A)].

Expression, purification, and spin-labeling of N_{TAIL} variants

All recombinant N_{TAIL} proteins were expressed in *E. coli* and were recovered from the soluble fraction of bacterial lysates (data not shown). The N_{TAIL} mutated proteins were purified to homogeneity (>95%) in two steps: immobilized metal affinity chromatography and gel filtration. As shown in Figure 3, all the N_{TAIL} mutated proteins migrate in SDS-PAGE with an apparent MM of about 20 kDa (expected MM is ~14.6 kDa). This abnormal migratory behavior has already been documented for N_{TAIL}, where mass spectrometry analysis and N-terminal sequencing gave the expected results.[21] This anomalous electrophoretic mobility is rather due to a relatively high content of acidic residues, as frequently observed in IDPs.[2] Likewise, the behavior of the mutated N_{TAIL} proteins can be accounted for by this sequence bias composition.

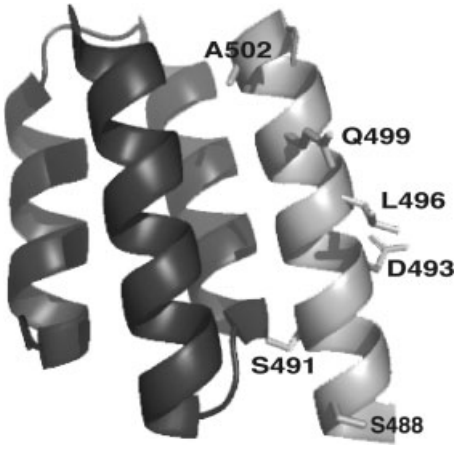

Figure 2

Ribbon representation of the crystal structure of the chimera between XD and the N_{TAIL} region encompassing residues 486–504 (pdb code 1T60) showing the orientation of the side chains of residues targeted for cysteine substitution and spin labeling. Note that the side chain of residue 491 points towards the surface of XD, while all the other side chains are solvent-exposed. The picture was drawn using Pymol (DeLano, W.L. The PyMOL Molecular Graphics System (2002) DeLano Scientific, San Carlos, CA, USA,. http://www.pymol.org).

In the case of the Q499C and A502C variants, a protein band of ~36 kDa is also observed in SDS-PAGE (Fig. 3). This band corresponds to a dimeric, disulfide-bridged form of the protein, as judged from its disappearance upon reduction with a one thousand-fold molar excess of DTT (data not shown).

The Stokes radius (R_S) value of the N_{TAIL} mutated proteins, as inferred from gel filtration, is close to that observed for *wt* N_{TAIL} (data not shown). The corresponding hydrodynamic volume of N_{TAIL} proteins is consistent with the theoretical value expected for a premolten globule state,[3] as already observed in the case of *wt*

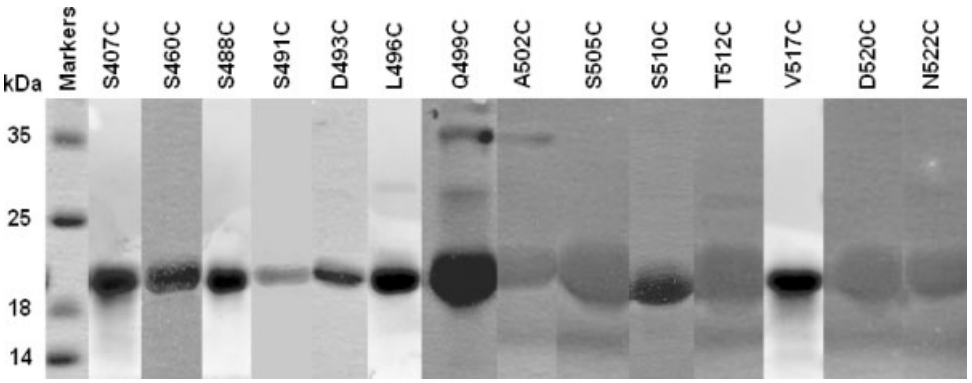

Figure 3

Coomassie blue staining of a 12% SDS-PAGE loaded with N_{TAIL} mutated proteins purified from the soluble fraction of *E. coli*. M: molecular mass markers.

N_{TAIL}.[21] Thus, these mutated proteins share similar hydrodynamic properties with *wt* N_{TAIL}, being all non-globular while possessing a certain residual compactness typical of the premolten globule state.[41]

The purified N_{TAIL} variants were successively spin-labeled through a two-step procedure consisting of a DTT reduction followed by covalent modification of the sulfydryl group by the MTSL nitroxide derivative as described in Ref. 24. In the case of the Q499C and A502C variants, a one thousand-fold molar excess of DTT was used to ensure reduction of the intermolecular disulfide bridge prior to spin labeling. Labeling yields ranged from 50 to 80%. Differences in labeling yields were not position-dependent and were ascribed to more subtle differences in the experimental conditions rather than to a different extent of solvent-exposure of the sulfydryl group, in agreement with the prevalently unfolded state of N_{TAIL}.

Analysis of structural propensities of N_{TAIL} variants by CD

A crucial point for further analysis, was to assess whether the cysteine substitution and the introduction of the covalently bound nitroxide radical could affect the overall secondary structure content of the various N_{TAIL} variants. Notably, secondary structure predictions using Psipred[46] point out no differences amongst the various N_{TAIL} variants, with an α-helix spanning residues 491–502 being predicted as the sole secondary structure element in all cases (data not shown). The far-UV CD spectra of spin-labeled N_{TAIL} proteins variants at neutral pH quite well superimpose onto that of *wt* N_{TAIL}, and are all typical of unstructured proteins, as seen by their large negative ellipticity at 200 nm and moderate ellipticity at 190 nm [Fig. 4(A)]. These data indicate that the cysteine substitution and the introduction of the spin label induce little, if any, structural perturbations. In agreement, most spin-

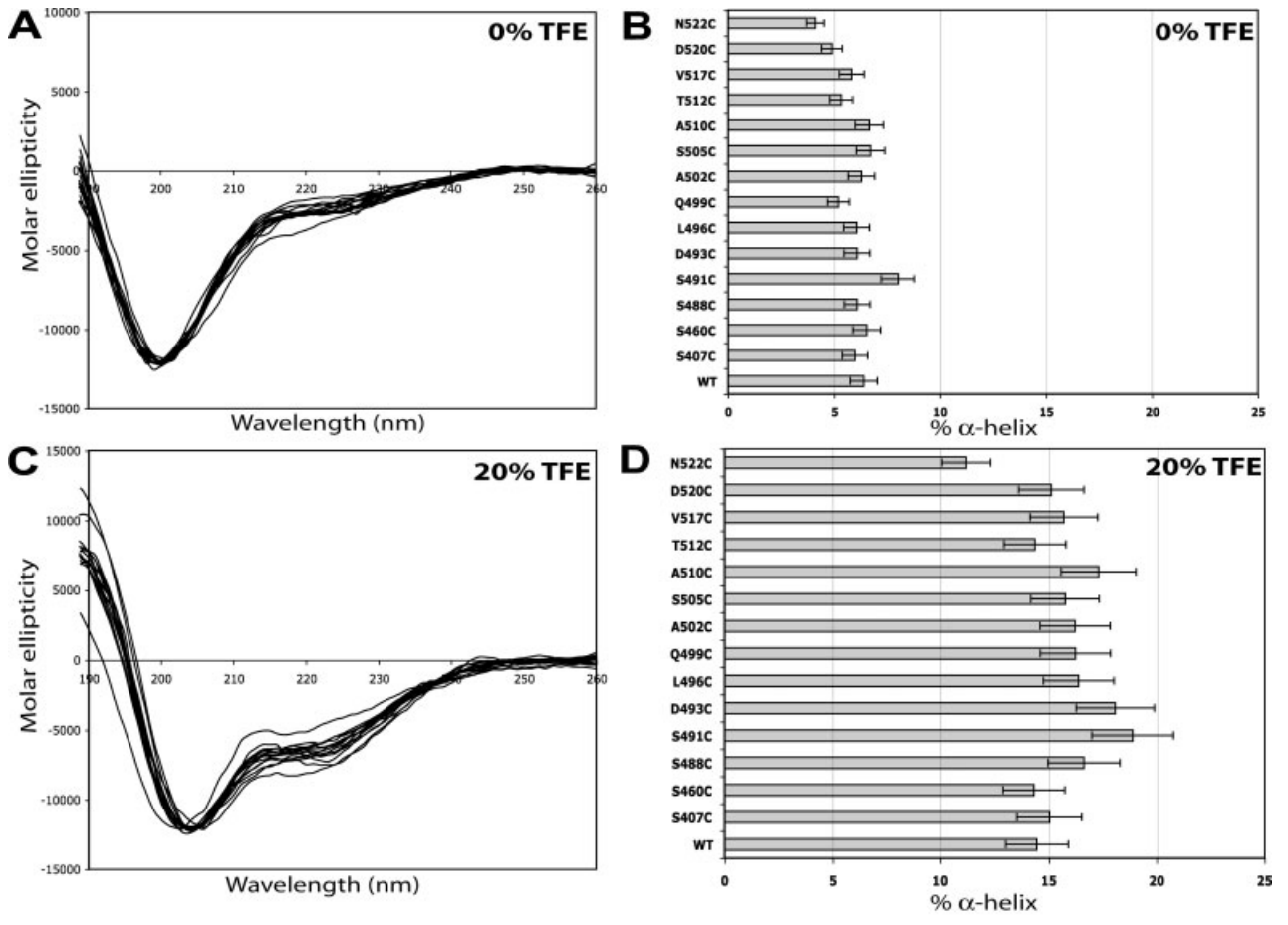

Figure 4

(**A, C**). CD spectra of spin-labeled and *wt* N_{TAIL} proteins at 0% (A) and 20% TFE (C). (**B, D**). α-helical content of spin-labeled and *wt* N_{TAIL} proteins at 0% (B) and 20% (D) TFE. Each spectrum is the mean of three independent acquisitions. The error bar (10% of the value) corresponds to the experimentally determined standard deviation from three independent experiments. The α-helical content was derived from the ellipticity at 222 nm as described in Ref. 44. For S407C, S488C, L496C, and V517C N_{TAIL} variants, see also Ref. 24.

labeled N_{TAIL} variants possess an α-helical content similar to that of *wt* N_{TAIL}. However, the N522C and the S491C variants exhibit, respectively, a slightly lower and higher α-helical content as compared to *wt* N_{TAIL} [Fig. 4(B)].

We also analyzed the structural propensities of the spin-labeled variants in the presence of 20% TFE. The TFE solvent mimics the hydrophobic environment experienced by proteins in protein-protein interactions and is therefore widely used as a probe to unveil disordered regions having a propensity to undergo an induced folding.[47] We previously reported that the addition of increasing amounts of TFE to N_{TAIL} triggers a gain of α-helicity, and that Box2/α-MoRE plays a major role in this α-helical transition.[14,21,32] We thus recorded CD spectra of all the spin-labeled N_{TAIL} proteins in the presence of 20% TFE [Fig. 4(C)] and calculated their α-helical content [Fig. 4(D)]. All proteins show a gain of α-helicity upon addition of TFE [Fig. 4(D)], thus indicating that neither the cysteine substitution nor the presence of the spin label impair the ability of N_{TAIL} to undergo α-helical folding. Notably, the α-helical propensity of spin-labeled S491C and D493C variants is slightly enhanced, as judged on the basis of their increased α-helical content at 20% TFE as compared to all the other spin-labeled N_{TAIL} variants and to native N_{TAIL} [Fig. 4(D)].

EPR data analysis of spin-labeled N_{TAIL} variants

In the absence of XD

For all the spin-labeled N_{TAIL} proteins, the EPR spectra are indicative of a high radical mobility, as judged on the basis of the $h(+1)/h(0)$ ratio (ranging from 0.83 to 0.98 ± 0.02) (Fig. 5, left and bottom panels). The EPR spectra exhibit a relatively narrow, single-component shape, with an outer line splitting of 3.22 (±0.02) mT (Fig. 5, left panel). Despite the overall high mobility, slight differences were observed in the different spin-labeled N_{TAIL} proteins. The label sites can be separated into two groups according to their $h(+1)/h(0)$ ratios: sites spanning positions 488–502, with a ratio centered at around 0.84, and all the other sites with a ratio higher than 0.88 (Fig. 5, bottom panel).

In the presence of XD

In order to investigate the folding events that N_{TAIL} undergoes in the presence of XD, we monitored EPR spectra of spin-labeled N_{TAIL} variants (100 μ*M*) in the presence of a molar excess of XD. For each variant, the molar excess of XD was progressively increased until saturation was achieved. Under saturating conditions, the extent of reduction of the mobility of the spin label is maximal, and further increasing the molar excess of XD does not result in any further variation in the radical mobility.

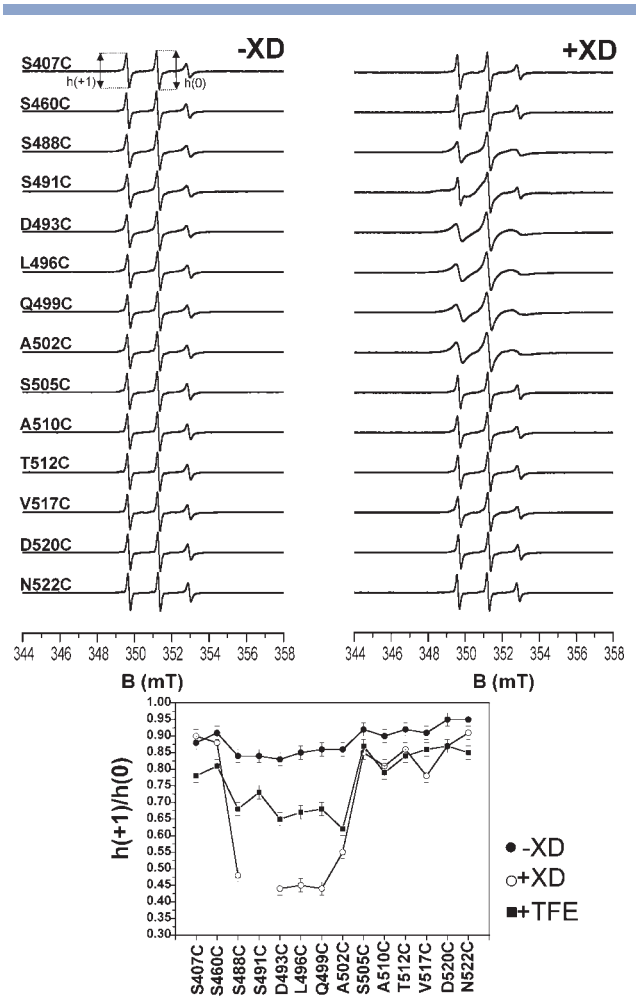

Figure 5

Amplitude normalized room temperature EPR spectra of the spin-labeled N_{TAIL} proteins (100 μ*M*) in the absence (left panel) or presence of a molar excess of XD (right panel). $h(+1)/h(0)$ ratios of the spin-labeled N_{TAIL} proteins free and in the presence of either saturating amounts of XD or 20% TFE as a function of spin-label position (bottom panel). Note that the $h(+1)/h(0)$ ratio of the spin-labeled S491C variant was not indicated, as it is not a reliable indicator of the mobility of this spin label (see text). For S407C, S488C, L496C, and V517C N_{TAIL} variants, see also Ref. 24.

In all cases, addition of stoichiometric amounts of XD are not sufficient to lead to saturation, with a two-fold molar excess of XD being required in most cases. Even larger XD molar excesses were required to achieve saturation in the case of spin-labeled Q499C and A502C (four-fold), and of S491C (eight-fold). It should be pointed out however, that we could not determine the K_D of the various spin-labeled N_{TAIL} variants, because in the range of 0–50% of N_{TAIL}-XD complex, the observed variations in the $[h(+1)/h(0)]_{mixture}$ ratio were within the error bar (data not shown). As a negative control, we recorded EPR spectra of a mixture containing spin-labeled L496C and an eight-fold molar excess of an irrelevant protein (lysozyme). No variation in the radical mobility was

observed (data not shown), thus indicating that the reductions in the radical mobility observed in the presence of XD are specific of complex formation.

The mobility of most spin labels is significantly reduced upon addition of XD, with the exception of spin labels grafted at positions 407 and 460, whose mobility is not affected even at XD molar excesses as high as eight (Fig. 5, right and bottom panels). The most dramatic reductions in the radical mobility are observed for the N_{TAIL} variants whose spin labels are located within the α-helix observed in the crystal structure of the XD/α–MoRE chimera, namely D493C, L496C, and Q499C, followed by S488C and A502C with variations in the $h(+1)/h(0)$ ratio of about 0.40 or 0.30, respectively (Fig. 5, bottom panel). In the case of S491C, addition of XD triggers a dramatic spectral change: the EPR spectrum is in fact drastically different and reflects a highly restricted nitroxide radical mobility, with a broad outer line splitting. This particular case will be discussed in more details in the paragraph "Effect of XD on the mobility of the spin label grafted at position 491."

On the other hand, the reduction in the mobility of the spin label grafted at positions 505 (i.e. at the end of Box2), 510 and 512 (region connecting Box2–Box3), 517 and 520 (Box3) is much less pronounced, with variations in $h(+1)/h(0)$ ratio of about 0.1 (Fig. 5, bottom panel). Position 522 is the least XD-sensitive, with a borderline decrease in the $h(+1)/h(0)$ ratio (Fig. 5, bottom panel).

Altogether these data indicate that the region spanning residues 488–520 is significantly affected by XD binding, while positions 407 (Box1) and 460 (middle of region connecting Box1–Box2) are not.

Effect of TFE on spin label mobility

We also recorded EPR spectra of spin-labeled N_{TAIL} proteins in the presence 20% TFE, a condition where all spin-labeled N_{TAIL} variants were shown to gain α-helicity (see Fig. 4). The addition of TFE triggers a decrease in the mobility of all spin labels (Fig. 5, bottom panel). The possibility that TFE could affect the mobility of the free radical in solution was checked and ruled out, by comparing the EPR spectra obtained with a 40 μ*M* MTSL solution in the presence or absence of 40% TFE (data not shown). Hence, the variations in the radical mobility observed in the presence of TFE with the spin-labeled N_{TAIL} proteins reflect changes in the protein environment in the proximity of the spin label. The most pronounced decrease in mobility is observed for the spin labels grafted in the 488–502 region, with mean variations in the $h(+1)/h(0)$ ratio of ∼0.16 (±0.02) (Fig. 5, bottom panel). On the other hand, the mobility of radicals bound within the 505–522 region is only moderately affected by the addition of TFE, with the highest variation in the $h(+1)/h(0)$ being 0.10 (±0.02) (Fig. 5, bottom panel). Notably, addition of 20% TFE triggers a reduction in the mobility of the spin labels grafted within the 505–522 region comparable to that observed with XD, while for the 488–502 region the effect of XD is much more pronounced (Fig. 5, bottom panel). The same pattern was observed in the presence of 30% sucrose, although all mobilities were reduced (data not shown).

Equilibrium displacement experiments

The lack of significant variations in the mobility of a spin label upon addition of XD, can in principle be accounted for by assuming that either the spin-labeled N_{TAIL} protein has lost the ability to interact with XD, or that the interaction does occur but does not affect the radical mobility because the label is located outside the region of interaction. In the case of the spin-label grafted at position 407, we have already shown that the lack of variation in the radical mobility is due to the fact that the radical is not located in the region of the interaction, with the mutated S407C N_{TAIL} protein being able to interact with XD.[24] In order to assess whether the lack of significant variations in the mobility of the spin label grafted at position 460 upon addition of XD was due to inability of this N_{TAIL} variant to bind to XD, we carried out equilibrium displacement experiments. We have previously shown that complex formation with XD is a reversible process, meaning that *wt* N_{TAIL} can sequester XD from a complex with spin-labeled N_{TAIL}.[24] In order to assess whether the S460C variant has the same ability, we first "EPR-silenced" this variant by ascorbic acid reduction, which triggers the conversion of the nitroxide group into a hydroxylamine label that is "silent" in EPR spectroscopy. After removing ascorbic acid, we checked the ability of the reduced, hydroxylamine-labeled protein to displace the equilibrium of the complex formation between spin-labeled L496C N_{TAIL} and XD.

We first recorded the EPR spectrum of a mixture containing spin-labeled L496C N_{TAIL} and XD in the 1:2 molar ratio [Fig. 6(A)]. Under these conditions the percentage of N_{TAIL} bound to XD was estimated to be 100%, as judged from the spectral shape (see also Ref. 24). We then recorded the EPR spectrum of a mixture containing spin-labeled L496C, XD and the reduced, hydroxylamine-labeled form of S460C in the 1:2:1 molar ratio [Fig. 6(A)]. The rationale for the choice of these molar ratios resides in the observation that the highest variations in the $[h(+1)/h(0)]_{mixture}$ ratio occur in the range of percentages of N_{TAIL}-XD complex comprised between 60 and 100% [see Fig. 6(B) and Ref. 24]. The spectrum obtained in these experimental conditions is composed of two signals: one arising from the unbound spin-labeled L496C protein and one resulting from the spin-labeled L496C protein bound to XD. Under these conditions, the $[h(+1)/h(0)]_{mixture}$ is 0.73 (±0.02 [Fig. 6(A)]. This decrease indicates that XD can dissociate from spin-labeled L496C and can associate with hydroxylamine-labeled S460C.

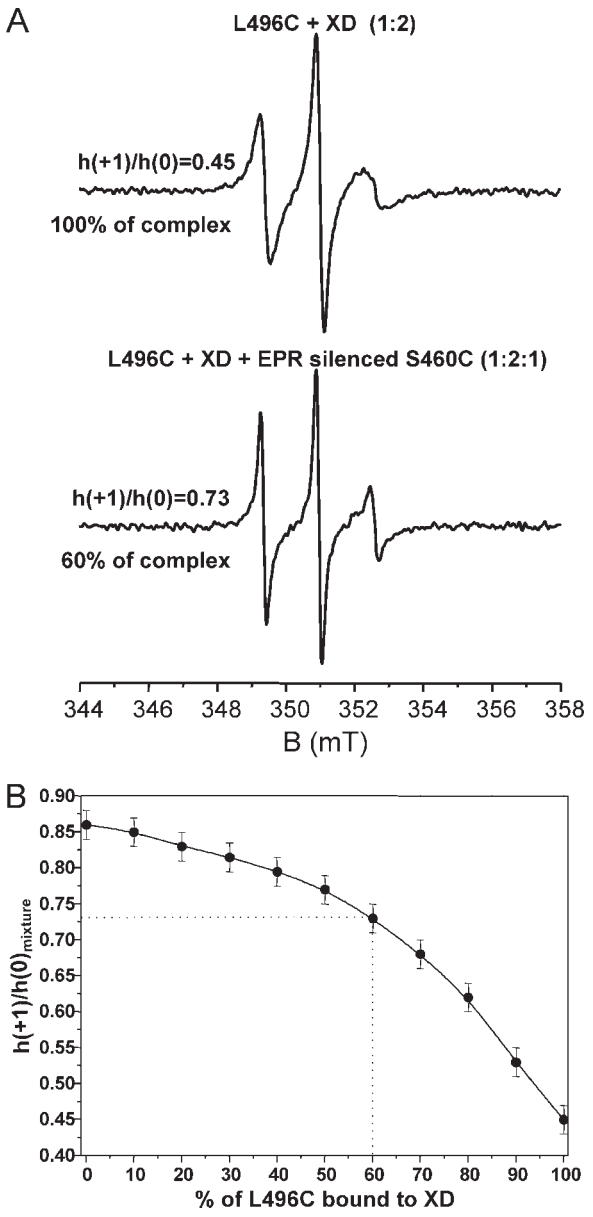

Figure 6

Dissociation of the spin-labeled S496C-XD complex by EPR-silenced S460C N_{TAIL}. (**A**) Amplitude normalized room temperature EPR spectra of the two mixtures. The molar ratios and the $h(+1)/h(0)$ ratios are also indicated. (**B**) Calibration curve allowing to infer the percentage of the spin-labeled L496C-XD complex from the $[h(+1)/h(0)]_{mixture}$ ratio (see Materials and Methods).

The percentage of spin-labeled L496C still bound to XD was inferred from the $[h(+1)/h(0)]_{mixture}$ ratio using a calibration curve obtained by calculating composite spectra corresponding to mixtures of recorded spectra of free and 100% XD-bound spin-labeled L496C [see Fig. 6(B)]. Addition of hydroxylamine-labeled S460C triggers a reduction in the percentage of bound L496C form from 100 to 60% ($\pm$5%) [Fig. 6(A)]. As a negative control, we recorded an EPR spectrum of a mixture containing spin-labeled L496C, XD and lysozyme in 1:2:1 ratio. No variation in the percentage of complex was observed (data not shown), reflecting lysozyme inability to interact with XD and to displace the equilibrium.

These results indicate that the hydroxylamine-labeled S460C N_{TAIL} variant is able to interact with XD. Therefore the lack of reduction in the mobility of the radical bound at position 460 upon addition of a molar excess of XD points out the absence of the involvement of this site in the interaction with XD.

Effect of sucrose on the spin label mobility

To further analyze the nature of the transition that the spin-labeled N_{TAIL} proteins undergo in the presence of XD, we recorded EPR spectra of the N_{TAIL} variants in the presence of 30% sucrose. Under these conditions, the contribution of protein rotation to the EPR spectral line shape is reduced due to an increase in the protein rotational correlation time by about a factor three. Moreover, it has been shown that the addition of 10–40% sucrose does not affect the rotational mobility of the side chain relative to the protein at room temperature.[45] The possibility that 30% sucrose might affect the overall secondary structure of the spin-labeled N_{TAIL} proteins was checked and ruled out by using CD (data not shown). As expected, the mobility of all spin labels was significantly reduced in the presence of sucrose (cf. Figs. 5 and 7, left panels) regardless of the position of the spin label. Upon addition of XD, the same pattern of variations in mobility is observed as in the absence of sucrose, with a dramatic impact of XD on the region spanning residues 488–502, modest impact on the region encompassing residues 505–520, borderline effect on position 522 and no significant impact on positions 407 and 460 (Fig. 7, bottom panel). The mobility of the nitroxide radicals of S488C, D493C, L496C, Q499C, and A502C N_{TAIL} variants bound to XD is in the twilight zone between the high and intermediate regime of mobility (with $\tau < 1$ ns). Conversely, in the case of the S491C variant a dramatic reduction in the radical mobility is observed (see paragraph "Effect of XD on the mobility of the spin label grafted at position 491").

Furthermore in the presence of XD, as already observed in the absence of sucrose (Fig. 5, bottom panel), a slightly higher mobility is observed for the spin label at positions 488 and 502 as compared to positions 493, 496, and 499 (Fig. 7, bottom panel). Conversely, the EPR spectra of all the other N_{TAIL} variants (i.e. S505C, S510C, T512C, V517C, and D520C) bound to XD do not exhibit this dramatic drop in the probe mobility, thus supporting lack of stable folding of the 505–522 region.

Effect of XD on the mobility of the spin label grafted at position 491

As already mentioned, a eight-fold molar excess of XD is required to achieve saturation in the case of the S491C

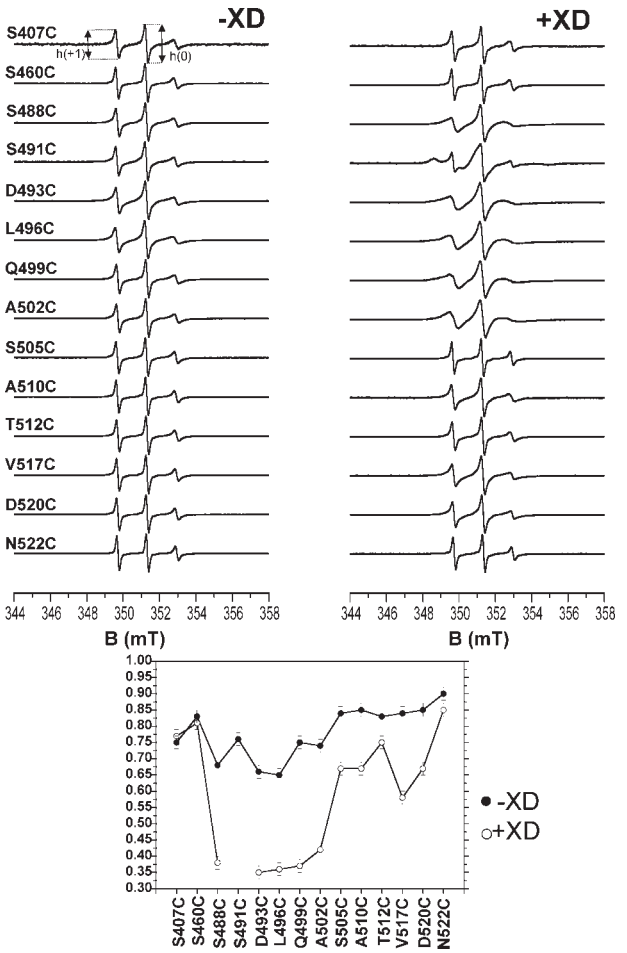

Figure 7

Amplitude normalized room temperature EPR spectra of the spin-labeled N_{TAIL} proteins (100 μ*M*) in the presence of 30% sucrose and in the absence (left panel) or presence of a molar excess of XD (right panel). $h(+1)/h(0)$ ratios of the spin-labeled N_{TAIL} proteins either free or in the presence of saturating amounts of XD as a function of spin-label position (bottom panel). Note that the $h(+1)/h(0)$ ratio of the spin-labeled S491C variant was not indicated, as it is not a reliable indicator of the mobility of this spin label (see text). For S407C, S488C, L496C, and V517C N_{TAIL} variants, see also Ref. 24.

N_{TAIL} variant, thus pointing out its reduced affinity towards XD with respect to all other variants (Fig. 8, left panel). Contrary to all other spin-labeled N_{TAIL} variants, in the case of the S491C variant, saturation does not correspond to 100% of bound form. Indeed, the experimentally observed EPR spectrum is composed of two signals: one arising from the unbound spin-labeled protein and one resulting from the spin-labeled protein bound to XD. The percentages of the free and bound form were estimated to be 25% ± 5% and 75% ± 5%, respectively (see Materials and Methods).

In agreement with the location of the radical buried at the N_{TAIL}-XD interface according to the chimera structure (see Fig. 2), the EPR spectrum obtained in the presence of saturating amounts of XD is typical of a highly restricted mobility of the spin label, as judged by the appearance of a novel spectral lineshape with a broader outer line splitting (5.95 ± 0.05 mT) as compared to the unbound form (3.22 ± 0.02 mT) (Fig. 8, left panel). As expected, the restriction of mobility is even more pronounced in the presence of 30% sucrose, where the mobility of the radical is severely restricted and the outer line splitting increases from 3.22 ± 0.02 mT to 6.35 ± 0.05 mT upon addition of XD (Fig. 8, right panel).

DISCUSSION

Despite the considerable body of information on the N_{TAIL}-XD interaction accumulated in the last years, (for reviews see Refs. [34–36]) the structural data available before this study was undertaken only concerned either crystallographic studies on a chimeric construct containing a short segment of N_{TAIL} or low-resolution SAXS data. We therefore studied the conformational change that N_{TAIL} undergoes in solution in the presence of XD by using SDSL EPR spectroscopy, a powerful technique that provides information at the residue level.

XD-induced folding of spin-labeled N_{TAIL} variants

In all cases, addition of stoichiometric amounts of XD are not sufficient to lead to saturation. Since the working concentration of spin-labeled N_{TAIL} variants was 100 μ*M*, requirement for XD molar excess indicates that the spin-labeled N_{TAIL} variants have a reduced affinity towards XD as compared to *wt* N_{TAIL}, whose reported K_D for XD is 100 n*M*.[14] In addition, the various spin-labeled N_{TAIL} variants display significant differences in their apparent affinity as a function of the radical location, with the grafting of the spin label at position 491 resulting in the most pronounced reduction in the apparent affinity. Interestingly, the grafting of the nitroxide radical at this position does not suppress complex formation but impairs the ability of the protein to yield 100% complex formation under the experimental conditions we used. Notably, the inability of spin-labeled S491C to bind to XD at 100% under saturating conditions, suggests that two protein populations can occur in solution, one of which (25%) would be unable to bind to XD even at over-saturating XD concentrations. We can speculate that these two populations may reflect static disorder, that is two alternate conformations of the side chain in position 491 (and hence of the spin label) with an occupancy of 0.75 and of 0.25. In the less populated one, the spin label would occur in a spatial position that would cause steric hindrance thereby preventing formation of a complex with XD. That IDPs might adopt distinct, unrelated conformations within the complexes they form with their

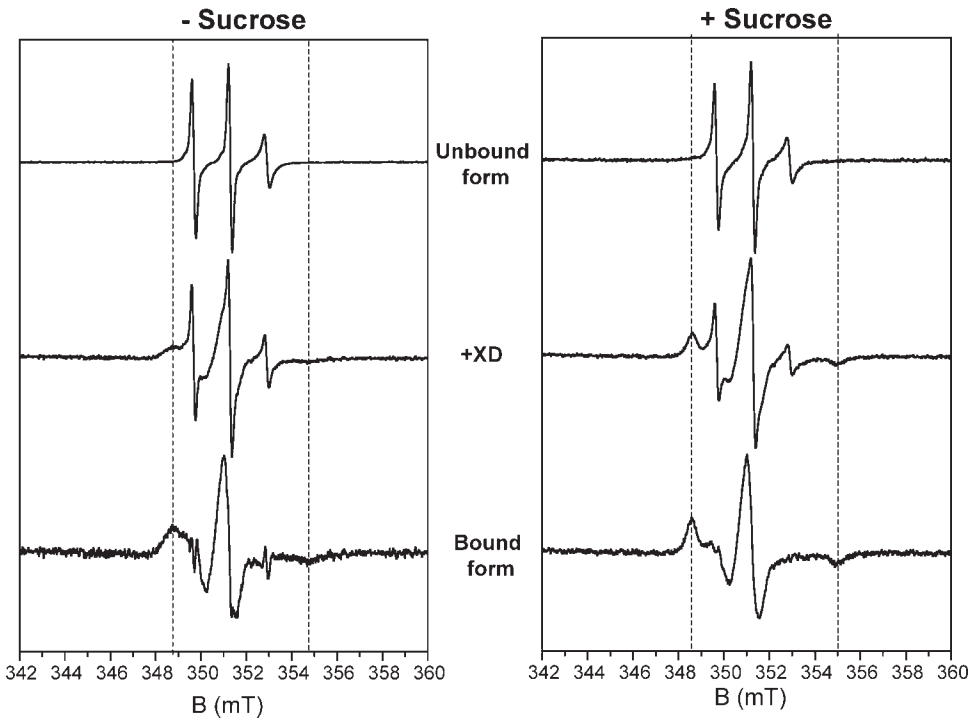

Figure 8

Amplitude normalized room temperature EPR spectra of the spin-labeled S491C N_{TAIL} protein (100 μ*M*) in the absence (left panel) or presence (right panel) of 30% sucrose either in the absence (top) or in the presence of saturating amounts of XD (middle). The EPR spectra shown at the bottom were obtained upon subtraction of the spectrum of the unbound form. The dotted lines indicate the outer line splitting for the bound form.

partners has been already reported (see Ref. 48 and references therein cited).

The lack of XD effect on the mobility of the spin label grafted at position 460 indicates that this latter position, like position 407, is not involved in the interaction either. This observation is in agreement with SAXS studies, which showed that the region upstream Box2 constitutes a flexible appendage.[14] Based on the results herein presented, we therefore can rule out the possibility that the region connecting Box1–Box2 may establish transient contacts with XD.

Conversely, addition of XD has a dramatic or moderate effect on the mobility of the spin labels grafted within the 488–502 and the 505–520 region, respectively. The "mobility" of a spin label grafted on a protein reflects several types of motion: movement of the entire protein, local backbone fluctuations, and internal dynamics of the spin-labeled lateral chain. In addition, motion can be restrained by possible tertiary contacts and by steric hindrance. In this study, except for position 491, the pattern of spin label mobilities in the 488–502 region in the presence of XD is the same as that observed in the presence of 20% TFE (see Fig 5 and below), thus indicating that the observed drop in the mobility is not due to a steric hindrance brought by XD. Moreover, an illustrative example of steric hindrance effect is provided by the spin-labeled N_{TAIL} S491C variant, where the motion of the label is dramatically reduced (see Fig. 8). This dramatic drop in mobility is consistent with the crystallographic structure of the chimera where the position 491 points towards XD and the space of the label at this site is embedded between the four helices of the complex.[33] The good agreement between crystallographic and EPR data suggests that the crystal structure of the chimera is a good model for the structure of the complex formed by XD and the entire N_{TAIL} in solution.

That the observed variations in spin label mobility in the presence of XD likely arise from a concerted movement of the backbone possibly also coupled to a variation in the side chain motion, rather than from a variation in this latter motion only, is supported by previous spectroscopic studies showing that Box2 undergoes α-helical folding upon binding to XD.[14,32,33] Similar conclusions have been drawn by Columbus and Hubbell who investigated the DNA-induced α-helical folding of GCN4 by using a similar SDSL approach.[49,50]

We then used 30% sucrose in order to dampen the contribution of the entire protein mobility to the EPR spectra by increasing the viscosity of the medium. Under these conditions, the spectra obtained for N_{TAIL} variants bearing the spin label grafted within the 488–502 region are reminiscent of those observed with spin-labeled variants of

proteins in which the radicals have been grafted at the surface of helices.[45,50] Taking also into account the fact that previous studies have shown that the XD-induced folding of N_{TAIL} implies the formation of an α-helix within the Box2 region,[14,32,33] the EPR data herein presented are consistent with the formation of an α-helix in the 488–502 region induced by the presence of XD.

In further support of this hypothesis, the drop in the radical mobility for the N_{TAIL} variants whose radical is grafted within the 488–502 region is much more pronounced than that of variants in which the spin label is bound to the downstream region.

Interestingly, a slightly higher mobility is observed for the spin labels bound to positions 488 and 502 as compared to positions 493, 496, and 499, regardless of whether sucrose was added or not (see Figs. 5 and 7, bottom panels). This difference may reflect a more constrained motion of the spin labels in the central part of the α-MoRE. That the extremities of α-helices are more mobile than their central parts has already been well documented by SDSL EPR spectroscopy.[45]

Finally, a borderline reduction is observed for the mobility of the spin label grafted at position 522 in the presence of XD, indicating that this residue remains highly flexible within the complex.

Residual structure within N_{TAIL}

Analysis of the EPR spectra of spin-labeled N_{TAIL} variants in the absence of XD, points out the existence of significant differences in mobility as a function of the spin label position, with the most reduced mobility being observed for the spin labels grafted within the 488–502 region. These differences in mobility could reflect differences in the content of transient secondary structure elements in the local environment experienced by each label, in agreement with previous observations pointing out that N_{TAIL}, is not a uniform random-coil, but rather belongs to the premolten globule sub-family,[21] with Box2 undergoing α-helical folding upon binding to XD.[24,31–33] Accordingly, the flexibility of Box2 may be restrained by the occurrence of a fluctuating α-helix, which would be transiently populated even in the absence of the partner. To ascertain the presence of this residual, fluctuating α-helix within the 488–502 region of N_{TAIL}, we recorded EPR spectra in the presence of 8*M* urea (data not shown and Ref. 24). No significant variations in the spin label mobility were found between native and denaturing conditions, with the only exception of the spin labels grafted to positions 488 and 496 positions for which borderline variations were observed (data not shown and Ref. 24) Nevertheless, slightly higher $h(+1)/h(0)$ ratios were measured in the 488–502 region. However, the observed variations were within the error bar, due to the very high mobility of the spin labels already observed in native conditions. Taking into account the fact that the 486–502 region of N_{TAIL} adopts an α-helical conformation upon binding to XD, as judged on the basis of both crystallographic[33] and EPR studies, (see also Ref. 24) the lower mobility of the spin-labels grafted within Box2 may reflect the predominance of an α-helical conformation among the highly fluctuating conformations sampled by unbound N_{TAIL}. That the conformational space of MoREs[18,51–53] in the unbound state is restricted by their inherent conformational propensities, thereby reducing the entropic cost of binding, has already been proposed.[2,11,17,52–54]

Effect of α-helical folding of Box2 on the downstream region

Experiments in the presence of sucrose showed that addition of XD does not trigger a transition to a folded state within the 505–522 region of N_{TAIL}. The slight drop in the mobility of the spin labels grafted within this region observed upon addition of XD could be ascribed either to a gain of rigidity arising from α-helical folding of the neighboring Box2 region or to the presence of XD, which might restrain the conformational space available to the radicals grafted within the C-terminal region of N_{TAIL}. To discriminate among these hypotheses, we monitored the gain of rigidity that N_{TAIL} undergoes in the presence of 20% TFE, a condition where the impact of the α-helical folding of Box2 upon the mobility of the radicals grafted downstream can be assessed and separated from the effect due to complex formation with XD. Addition of TFE triggers a decrease in the mobility of the spin labels bound within the 505–522 region that is comparable to that induced by XD. Taking also into account the fact that TFE does not promote α-helical folding within Box3,[14] these data suggest that the α-helical transition taking place within Box2, is responsible for the restrained motion of the downstream region, rather than a direct interaction with XD. On the other hand, the reduction in the mobility of the spin labels grafted in the 488–502 region is more pronounced in the presence of XD than in the presence of 20% TFE (Fig. 5, bottom panel). This difference can likely be ascribed to the ability of XD to stabilize the formation of the α-MoRE, while this latter would be only transiently populated in the unbound form of N_{TAIL} in the presence of TFE.

The more pronounced effect of TFE on the mobility of spin labels grafted within the 488–502 region with respect to the downstream region, also indicates that TFE does not promote non native folding within N_{TAIL}, thus confirming and extending our previous data[24] pointing out the reliability and biological relevance of structural information provided by studies making use of this secondary structure stabilizer.

Addition of TFE also promotes a drop in the mobility of the spin labels located outside the region of interaction with XD, namely positions 407 and 460 (see also Ref. 24). We have already proposed[24] that the biological

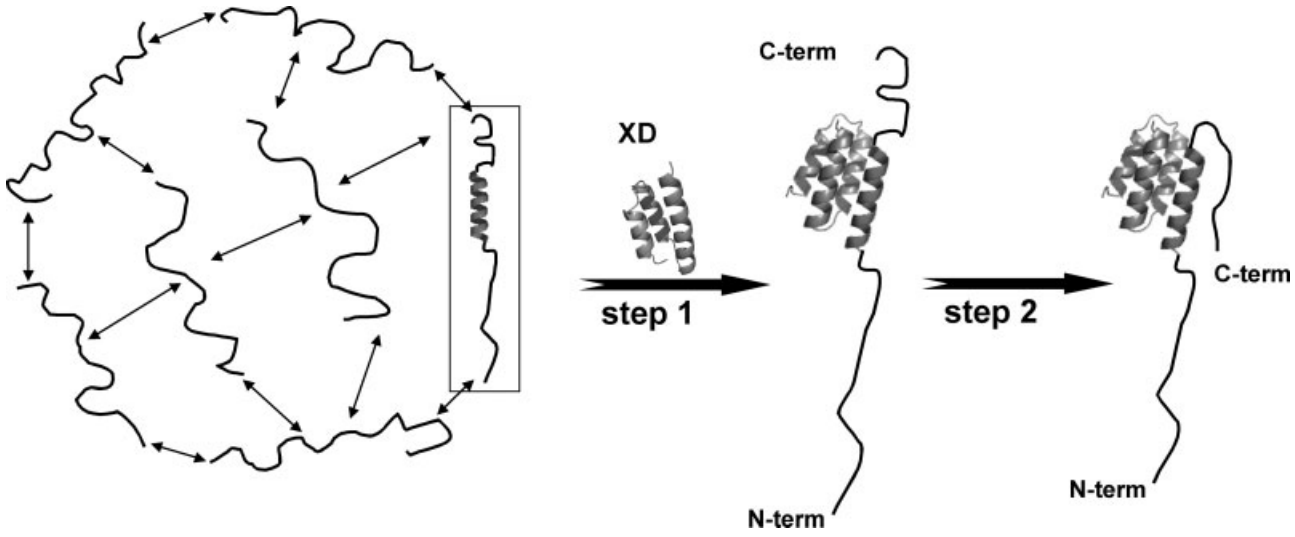

Figure 9

Schematic representation of the proposed molecular mechanism of the XD-induced folding of N_{TAIL} pointing out conformer selection by the partner and α-helical folding of the 488–502 region (helix) (Step 1), followed by establishment of tertiary contacts between Box2 and the downstream region (Step 2). Sequestration of the partially folded N_{TAIL} conformer by the partner will result in a shift in the equilibrium amongst N_{TAIL} conformers progressively leading to full complex formation with XD.

relevance of the folding propensity of Box1 may be related to a possible gain of structure induced by binding of the Nucleoprotein Receptor to Box1.[27,28] We can speculate that the TFE-induced gain of rigidity of the nitroxide label grafted at position 460 might either reflect an intrinsic local, structural propensity, or arise from a gain of rigidity of the neighboring Box1 and/or Box2 regions. Further studies, implying introduction of spin labels scattered in the region upstream Box2 would be required to address this point.

CONCLUSION

In conclusion, using SDSL EPR spectroscopy we mapped the N_{TAIL} region involved in α-helical folding in solution. We showed that different N_{TAIL} regions contribute to a different extent to the folding process induced by XD. We also showed that the interaction between N_{TAIL} and XD implies the stabilization of the helical conformation of the α-MoRE, which is otherwise only transiently populated in the unbound form. The occurrence of a transiently populated α-helix even in the absence of the partner, suggests that the molecular mechanism governing the folding of N_{TAIL} induced by XD would rely on conformer selection (i.e. selection by the partner of a pre-existing conformation)[55,56] rather than on a "fly casting" mechanism,[57] contrary to what has been reported for the pKID-KIX couple.[58]

Stabilization of the helical conformation of the α-MoRE is also accompanied by a reduction in the mobility of the downstream region. The lower flexibility of the region downstream Box2 is not due to gain of α-helicity, nor can it be ascribed to a restrained motion brought by a direct interaction with XD. Rather, it likely arises from a gain of rigidity brought by α-helical folding of the neighboring Box2 region. In agreement with these data, preliminary titration studies using heteronuclear NMR, suggest that XD does not establish direct interactions with Box3 (Bernard et al., unpublished data), contrary to what has been previously proposed.[14]

We tentatively propose that binding to XD might take place through a sequential mechanism that could involve binding and α-helical folding of Box2, followed by a conformational change of Box3, whose overall mobility is consequently reduced probably through tertiary contacts with the neighboring Box2 region (see Fig. 9). That Box3 likely establishes contacts with Box2 is also supported by the SAXS-derived low-resolution model of the complex between N_{TAIL} and XD, which indicates that the C-terminus is not exposed to the solvent and is rather embedded in the globular, bulky part of the model accommodating XD and the α-MoRE [see Fig. 1(B) and Ref. 14]. The lower flexibility of the 505–520 region as compared with that of position 460 in the absence of the partner (see Fig. 5, bottom panel), also supports the ability of this region to establish transient, long-range contacts with other N_{TAIL} regions even in the absence of XD. Double spin-labeling experiments aimed at precisely determining

the location of Box3 with respect to other N_{TAIL} regions via distance measurements are in progress.

Finally, the large number of spin-labeled N_{TAIL} variants that we generated and their analysis by EPR spectroscopy provided us with a panel of spectral signatures that have a high predictive value. Indeed, the EPR spectral shape reflects the specific environment in the proximity of the spin label and the extent of involvement of the radical in the interaction with a partner, while providing information on possible α-helical transitions. As such, we will be able to infer information on the chemical environment and the implication of specific N_{TAIL} residues within complexes with other partners, such as the N_{TAIL}-Hsp72 and N_{TAIL}-IRF3 complexes for which no structural information is presently available.

ACKNOWLEDGMENTS

The authors thank Jean-Marie Bourhis, Coralie Attias, Matteo Colombo, and Guillaume Setrick (AFMB laboratory) for their contribution to cloning and spin-labeling procedures, as well as Sébastien Ranaldi and Ahmad Allouch (BIP laboratory) for their help in spin-labeling. They are also grateful to Frédéric Carrière (EIPL laboratory, UPR 9025-CNRS, Marseille, France) for stimulating discussions and for critical reading of the manuscript.

REFERENCES

1. Dunker AK, Lawson JD, Brown CJ, Williams RM, Romero P, Oh JS, Oldfield CJ, Campen AM, Ratliff CM, Hipps KW, Ausio J, Nissen MS, Reeves R, Kang C, Kissinger CR, Bailey RW, Griswold MD, Chiu W, Garner EC, Obradovic Z. Intrinsically disordered protein. J Mol Graph Model 2001;19:26–59.
2. Tompa P. Intrinsically unstructured proteins. Trends Biochem Sci 2002;27:527–533.
3. Uversky VN. Natively unfolded proteins: a point where biology waits for physics. Protein Sci 2002;11:739–756.
4. Tompa P. The functional benefits of disorder. J Mol Struct (Theochem) 2003;666/667:361–371.
5. Fink AL. Natively unfolded proteins. Curr Opin Struct Biol 2005;15:35–41.
6. Dyson HJ, Wright PE. Intrinsically unstructured proteins and their functions. Nat Rev Mol Cell Biol 2005;6:197–208.
7. Uversky VN, Oldfield CJ, Dunker AK. Showing your ID: intrinsic disorder as an ID for recognition, regulation and cell signaling. J Mol Recognit 2005;18:343–384.
8. Kriwacki RW, Hengst L, Tennant L, Reed SI, Wright PE. Structural studies of p21Waf1/Cip1/Sdi1 in the free and Cdk2-bound state: conformational disorder mediates binding diversity. Proc Natl Acad Sci USA 1996;93:11504–11509.
9. Uversky VN. What does it mean to be natively unfolded? Eur J Biochem 2002;269:2–12.
10. Dyson HJ, Wright PE. Coupling of folding and binding for unstructured proteins. Curr Opin Struct Biol 2002;12:54–60.
11. Fuxreiter M, Simon I, Friedrich P, Tompa P. Preformed structural elements feature in partner recognition by intrinsically unstructured proteins. J Mol Biol 2004;338:1015–1026.
12. Dunker AK, Cortese MS, Romero P, Iakoucheva LM, Uversky VN. Flexible nets. FEBS J 2005;272:5129–5148.
13. Fletcher CM, McGuire AM, Gingras AC, Li H, Matsuo H, Sonenberg N, Wagner G. 4E binding proteins inhibit the translation factor eIF4E without folded structure. Biochemistry 1998;37:9–15.
14. Bourhis JM, Receveur-Bréchot V, Oglesbee M, Zhang X, Buccellato M, Darbon H, Canard B, Finet S, Longhi S. The intrinsically disordered C-terminal domain of the measles virus nucleoprotein interacts with the C-terminal domain of the phosphoprotein via two distinct sites and remains predominantly unfolded. Protein Sci 2005;14:1975–1992.
15. Dunker AK, Obradovic Z. The protein trinity–linking function and disorder. Nat Biotechnol 2001;19:805–806.
16. Bienkiewicz EA, Adkins JN, Lumb KJ. Functional consequences of preorganized helical structure in the intrinsically disordered cell-cycle inhibitor p27(Kip1). Biochemistry 2002;41:752–759.
17. Lacy ER, Filippov I, Lewis WS, Otieno S, Xiao L, Weiss S, Hengst L, Kriwacki RW. p27 binds cyclin-CDK complexes through a sequential mechanism involving binding-induced protein folding. Nat Struct Mol Biol 2004;11:358–364.
18. Fuxreiter M, Tompa P, Simon I. Local structural disorder imparts plasticity on linear motifs. Bioinformatics 2007;23:950–956.
19. Karlin D, Longhi S, Canard B. Substitution of two residues in the measles virus nucleoprotein results in an impaired self-association. Virology 2002;302:420–432.
20. Kingston RL, Walter AB, Gay LS. Characterization of nucleocapsid binding by the measles and the mumps virus phosphoprotein. J Virol 2004;78:8615–8629.
21. Longhi S, Receveur-Brechot V, Karlin D, Johansson K, Darbon H, Bhella D, Yeo R, Finet S, Canard B. The C-terminal domain of the measles virus nucleoprotein is intrinsically disordered and folds upon binding to the C-terminal moiety of the phosphoprotein. J Biol Chem 2003;278:18638–18648.
22. Heggeness MH, Scheid A, Choppin PW. Conformation of the helical nucleocapsids of paramyxoviruses and vesicular stomatitis virus: reversible coiling and uncoiling induced by changes in salt concentration. Proc Natl Acad Sci USA 1980;77:2631–2635.
23. Heggeness MH, Scheid A, Choppin PW. The relationship of conformational changes in the Sendai virus nucleocapsid to proteolytic cleavage of the NP polypeptide. Virology 1981;114:555–562.
24. Morin B, Bourhis JM, Belle V, Woudstra M, Carrière F, Guigliarelli B, Fournel A, Longhi S. Assessing induced folding of an intrinsically disordered protein by site-directed spin-labeling EPR spectroscopy. J Phys Chem B 2006;110:20596–20608.
25. Zhang X, Glendening C, Linke H, Parks CL, Brooks C, Udem SA, Oglesbee M. Identification and characterization of a regulatory domain on the carboxyl terminus of the measles virus nucleocapsid protein. J Virol 2002;76:8737–8746.
26. Zhang X, Bourhis JM, Longhi S, Carsillo T, Buccellato M, Morin B, Canard B, Oglesbee M. Hsp72 recognizes a P binding motif in the measles virus N protein C-terminus. Virology 2005;337:162–174.
27. Laine D, Trescol-Biémont M, Longhi S, Libeau G, Marie J, Vidalain P, Azocar O, Diallo A, Canard B, Rabourdin-Combe C, Valentin H. Measles virus nucleoprotein binds to a novel cell surface receptor distinct from FcgRII via its C-terminal domain: role in MV-induced immunosuppression. J Virol 2003;77:11332–11346.
28. Laine D, Bourhis J, Longhi S, Flacher M, Cassard L, Canard B, Sautès-Fridman C, Rabourdin-Combe C, Valentin H. Measles virus nucleoprotein induces cell proliferation arrest and apoptosis through NTAIL/NR and NCORE/FcgRIIB1 interactions, respectively. J Gen Virol 2005;86:1771–1784.
29. Karlin D, Longhi S, Receveur V, Canard B. The N-terminal domain of the phosphoprotein of morbilliviruses belongs to the natively unfolded class of proteins. Virology 2002;296:251–262.
30. Karlin D, Ferron F, Canard B, Longhi S. Structural disorder and modular organization in Paramyxovirinae N and P. J Gen Virol 2003;84 (Part 12):3239–3252.
31. Johansson K, Bourhis JM, Campanacci V, Cambillau C, Canard B, Longhi S. Crystal structure of the measles virus phosphoprotein domain responsible for the induced folding of the C-terminal domain of the nucleoprotein. J Biol Chem 2003;278:44567–44573.

32. Bourhis J, Johansson K, Receveur-Bréchot V, Oldfield CJ, Dunker AK, Canard B, Longhi S. The C-terminal domain of measles virus nucleoprotein belongs to the class of intrinsically disordered proteins that fold upon binding to their pohysiological partner. Virus Res 2004;99:157–167.
33. Kingston RL, Hamel DJ, Gay LS, Dahlquist FW, Matthews BW. Structural basis for the attachment of a paramyxoviral polymerase to its template. Proc Natl Acad Sci USA 2004;101:8301–8306.
34. Bourhis JM, Canard B, Longhi S. Désordre structural au sein du complexe réplicatif du virus de la rougeole: implications fonctionnelles. Virologie 2005;9:367–383.
35. Bourhis JM, Canard B, Longhi S. Structural disorder within the replicative complex of measles virus: functional implications. Virology 2006;344:94–110.
36. Bourhis JM, Longhi S. Measles virus nucleoprotein: structural organization and functional role of the intrinsically disordered C-terminal domain. In: Longhi S, editor. Measles virus nucleoprotein. Hauppage, NY: Nova; 2007. pp 1–35.
37. Feix JB, Klug CS. Site-directed spin-labeling of membrane proteins and peptide-membrane interactions. In: Berliner L, editor. Inbiological magnetic resonance, Vol. 14. Spin Labeling: the next millenium. New York: Plenum; 1998. pp 251–281.
38. Hubbell WL, Gross A, Langen R, Lietzow MA. Recent advances in site-directed spin labeling of proteins. Curr Opin Struct Biol 1998;8:649–656.
39. Biswas R, Kuhne H, Brudvig GW, Gopalan V. Use of EPR spectroscopy to study macromolecular structure and function. Sci Prog 2001;84 (Part 1):45–67.
40. Belle V, Fournel A, Woudstra M, Ranaldi S, Prieri F, Thome V, Currault J, Verger R, Guigliarelli B, Carriere F. Probing the opening of the pancreatic lipase lid using site-directed spin labeling and EPR spectroscopy. Biochemistry 2007;46:2205–2214.
41. Uversky VN. Use of fast protein size-exclusion liquid chromatography to study the unfolding of proteins which denature through the molten globule. Biochemistry 1993;32:13288–13298.
42. Marsh D, Kurad D, Livshits VA. High-field electron spin resonance of spin labels in membranes. Chem Phys Lipids 2002;116:93–114.
43. Hubbell WL, McHaourab HS, Altenbach C, Lietzow MA. Watching proteins move using site-directed spin labeling. Structure 1996;4: 779–783.
44. Myers JK, Pace CN, Scholtz JM. Helix propensities are identical in proteins and peptides. Biochemistry 1997;36:10923–10929.
45. McHaourab HS, Lietzow MA, Hideg K, Hubbell WL. Motion of spin-labeled side chains in T4 lysozyme. Correlation with protein structure and dynamics. Biochemistry 1996;35:7692–7704.
46. McGuffin LJ, Bryson K, Jones DT. The PSIPRED protein structure prediction server. Bioinformatics 2000;16:404–405.
47. Hua QX, Jia WH, Bullock BP, Habener JF, Weiss MA. Transcriptional activator-coactivator recognition: nascent folding of a kinase-inducible transactivation domain predicts its structure on coactivator binding. Biochemistry 1998;37:5858–5866.
48. Tompa P, Fuxreiter M. Fuzzy complexes: polymorphism and structural disorder in protein-protein interactions. Trends Biochem Sci 2008;33:2–8.
49. Columbus L, Hubbell WL. A new spin on protein dynamics. Trends Biochem Sci 2002;27:288–295.
50. Columbus L, Hubbell WL. Mapping backbone dynamics in solution with site-directed spin labeling: GCN4-58 bZip free and bound to DNA. Biochemistry 2004;43:7273–7287.
51. Oldfield CJ, Cheng Y, Cortese MS, Romero P, Uversky VN, Dunker AK. Coupled folding and binding with alpha-helix-forming molecular recognition elements. Biochemistry 2005;44:12454–12470.
52. Mohan A, Oldfield CJ, Radivojac P, Vacic V, Cortese MS, Dunker AK, Uversky VN. Analysis of molecular recognition features (MoRFs). J Mol Biol 2006;362:1043–1059.
53. Vacic V, Oldfield CJ, Mohan A, Radivojac P, Cortese MS, Uversky VN, Dunker AK. Characterization of molecular recognition features. Mo RFs, and their binding partners J Proteome Res 2007;6:2351–2366.
54. Sivakolundu SG, Bashford D, Kriwacki RW. Disordered p27Kip1 exhibits intrinsic structure resembling the Cdk2/cyclin A-bound conformation. J Mol Biol 2005;353:1118–1128.
55. Tsai CD, Ma B, Kumar S, Wolfson H, Nussinov R. Protein folding: binding of conformationally fluctuating building blocks via population selection. Crit Rev Biochem Mol Biol 2001;36:399–433.
56. Tsai CJ, Ma B, Sham YY, Kumar S, Nussinov R. Structured disorder and conformational selection. Proteins 2001;44:418–427.
57. Shoemaker BA, Portman JJ, Wolynes PG. Speeding molecular recognition by using the folding funnel: the fly-casting mechanism. Proc Natl Acad Sci USA 2000;97:8868–8873.
58. Sugase K, Dyson HJ, Wright PE. Mechanism of coupled folding and binding of an intrinsically disordered protein. Nature 2007;447: 1021–1025.